Supporting Information

Z-Scheme BAIO/C_3N_4 Heterojunction Enabling Efficient Visible-Light Photocatalytic H_2O_2 Production via Direct One-Step Two-Electron O_2 Reduction Reaction

Kexin Yang,‡[a] Zhijia Song,‡[a] Xiaoxiao Fu,[a] Wei Yan,[a] Tao Zhang,[a] Yiwei Hua,[a] Haixin Lin,*[a,b] Qin Kuang *[a,b] and Zhaoxiong Xie [a,b]

[a] *State Key Laboratory of Physical Chemistry of Solid Surfaces, Collaborative Innovation Center of Chemistry for Energy Materials, Department of Chemistry, College of Chemistry and Chemical Engineering, Xiamen University, Xiamen 361005, China.*

[b] *Innovation Laboratory for Sciences and Technologies of Energy Materials of Fujian Province (IKKEM), Xiamen 361005, China.*

‡ *These authors contributed equally.*

* *Corresponding Authors.*

E-mail: qkuang@xmu.edu.cn, haixinlin@xmu.edu.cn

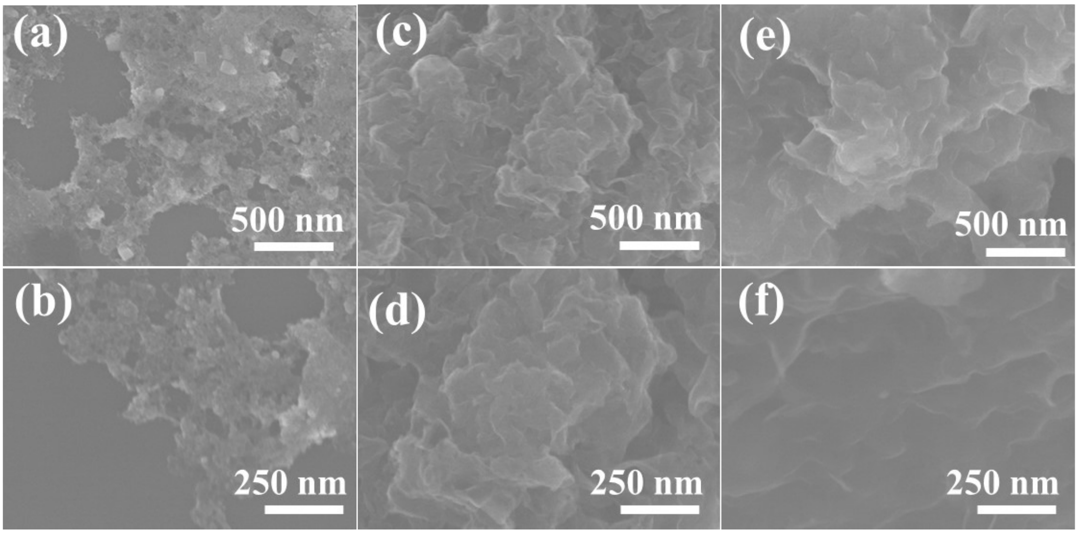

Figure S1 SEM images of (a, b) BAIO, (c, d) C_3N_4, and (e, f) BAIO/C_3N_4.

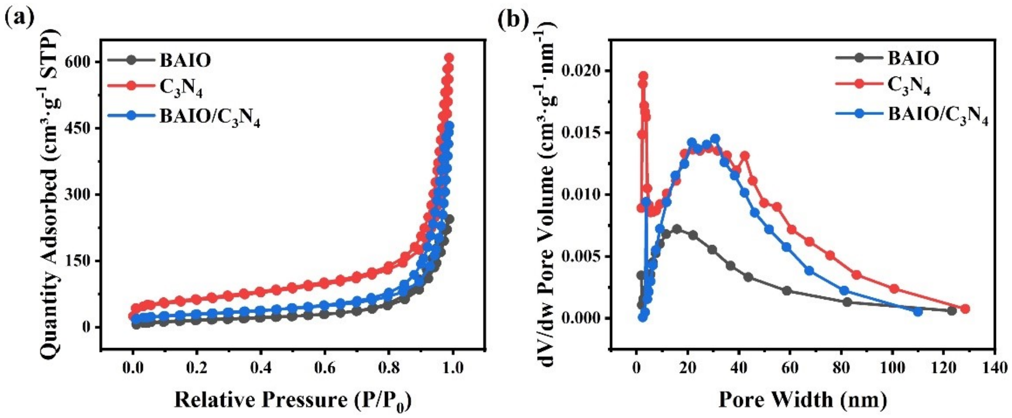

Figure S2 (a) N_2 adsorption-desorption isotherms and (b) corresponding BJH pore size distribution calculated from the desorption branch of the isotherms of BAIO, C_3N_4 and BAIO/C_3N_4.

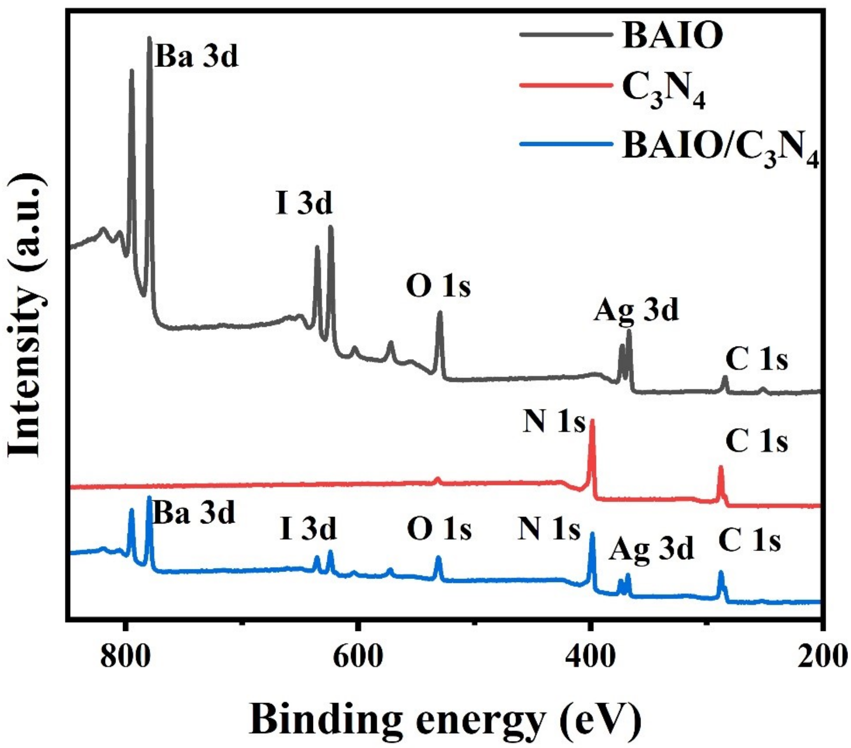

Figure S3 XPS spectra of survey scan in BAIO, C_3N_4 and BAIO/C_3N_4.

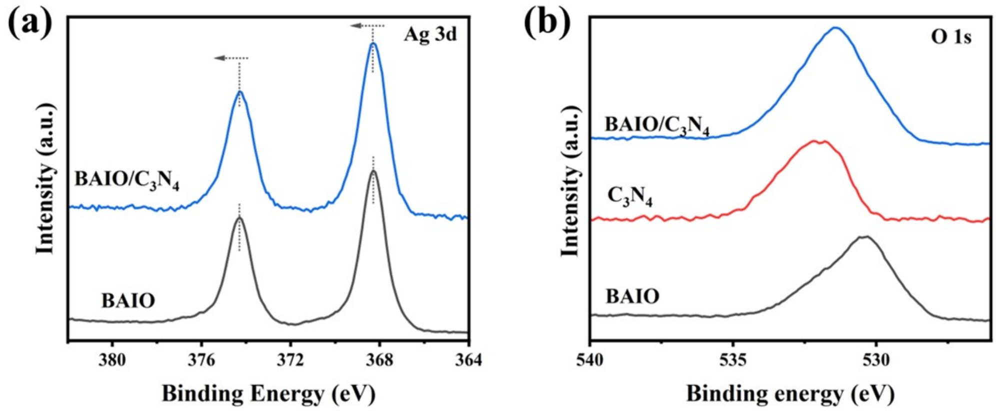

Figure S4 XPS spectra of (a) Ag 3d of BAIO and BAIO/C_3N_4. (b) O 1s XPS spectra of BAIO, C_3N_4 and BAIO/C_3N_4.

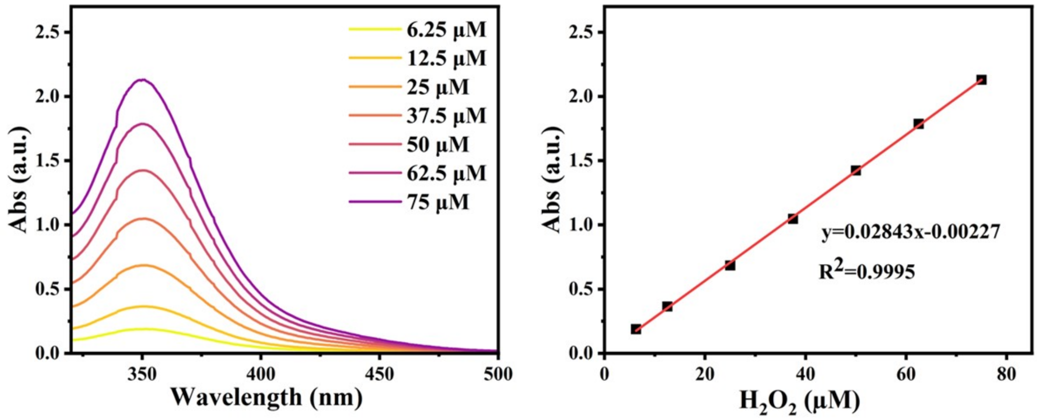

Figure S5 (a) Determination of UV-vis absorption intensity of different H_2O_2 concentrations by iodimetry. (b) The linear fitting formula of standard H_2O_2 concentration.

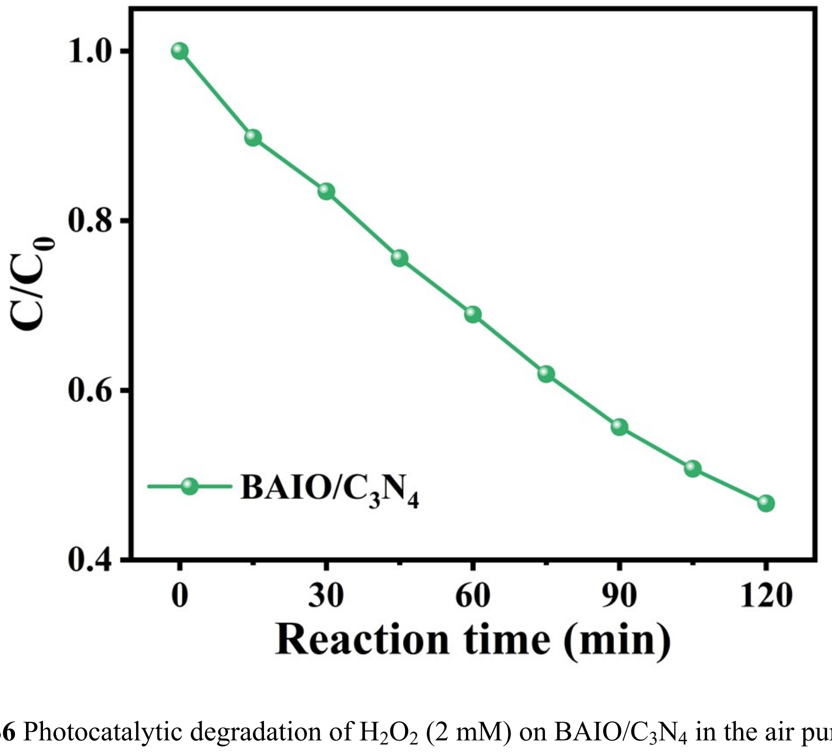

Figure S6 Photocatalytic degradation of H_2O_2 (2 mM) on $BAIO/C_3N_4$ in the air pure water.

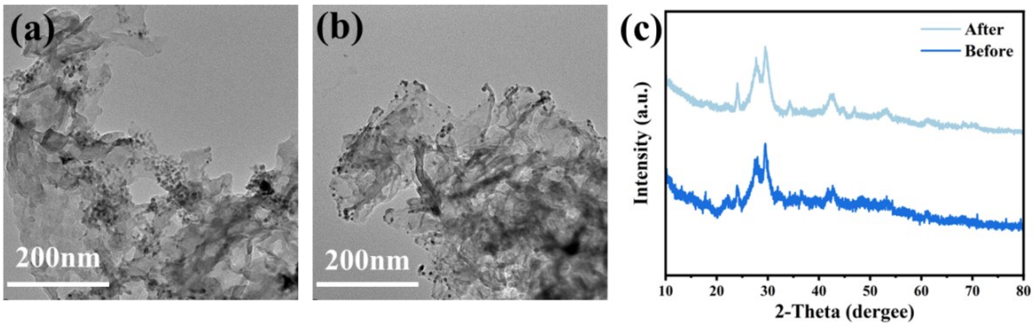

Figure S7 (a, b) TEM images and (c) XRD patterns of BAIO/C_3N_4 before and after photocatalytic H_2O_2 evolution.

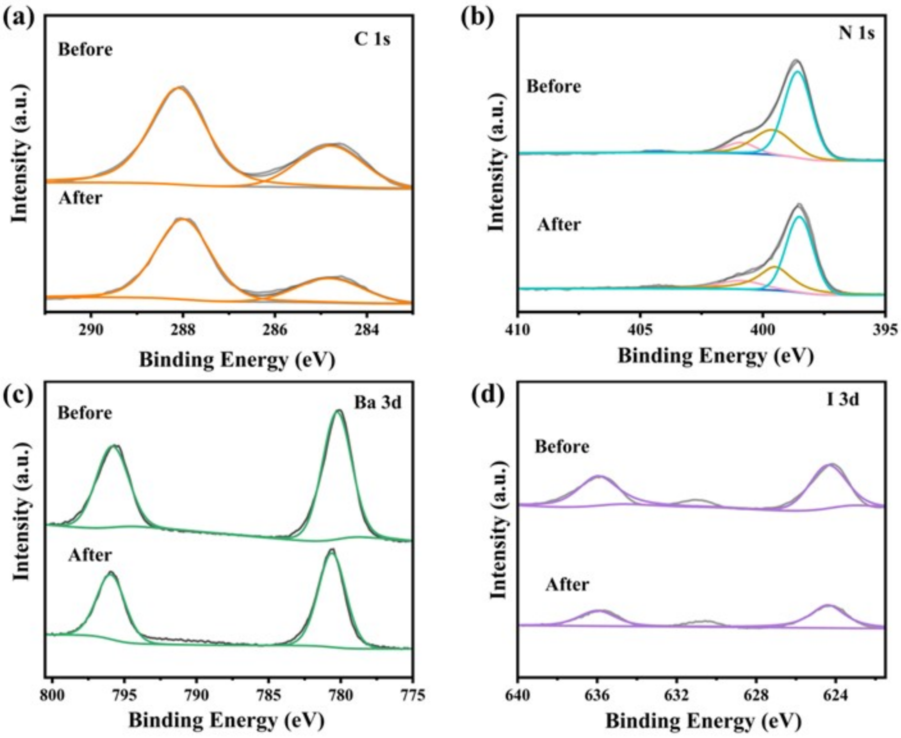

Figure S8 XPS spectra of BAIO/C_3N_4 before and after the photocatalytic H_2O_2 evolution: (a) C 1s, (b) N 1s, (c) Ba 3d and (d) I 3d.

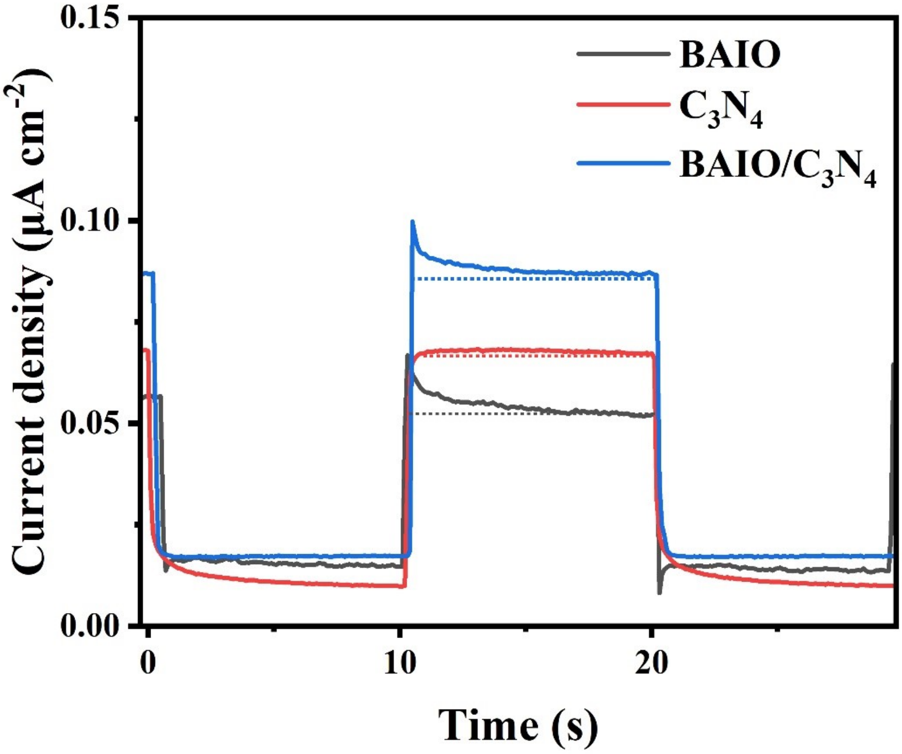

Figure S9 The transient photocurrent density of BAIO, C_3N_4 and BAIO/C_3N_4.

The built-in electric field (IEF) strength is calculated using the model formula proposed by Kanata et al., which is given by:

$$F_S = (-\frac{2\rho V_S}{\varepsilon\varepsilon_0})^{1/2}$$

Here, F_S represents the intensity of the built-in electric field (in V/cm), ρ is the surface charge density (in cm^{-2}), and *Vs* is the surface potential (in volts). $\varepsilon_0$and ε denote the vacuum permittivity and low-frequency permittivity, respectively, with ε_0 being a constant. For materials within the same class that exhibit similar structures and compositions, ε can be considered approximately constant. Therefore, only the surface charge density and surface potential need to be measured. The surface potential is determined by measuring the open-circuit potential of the material, while the surface charge density is derived from the transient photocurrent spectrum.

Consequently, the IEF values were calculated to be 1, 1.28, and 3.34 for BAIO,

C_3N_4, and BAIO/C_3N_4, respectively, with the intensity of BAIO normalized to "1" as a reference.

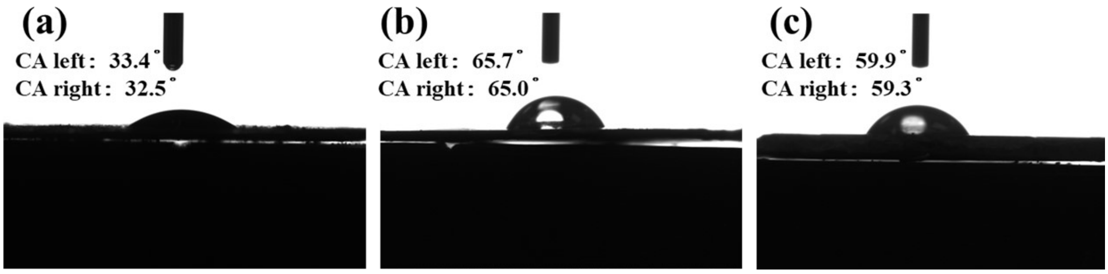

Figure S10 Water contact angle tests on the surface of (a) BAIO, (b) C_3N_4 and (c) BAIO/ C_3N_4.

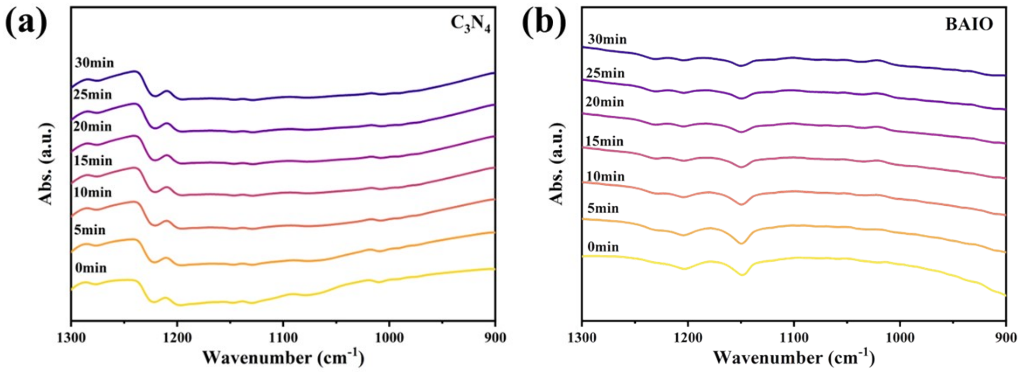

Figure S11 In situ DRIFTS spectra of BAIO and C_3N_4 for H_2O_2 production.

Table S1 Currently reported H_2O_2 yields for C_3N_4-based and heterojunction photocatalysts.

Materials	Reaction conditions	H_2O_2 yield (μmol g^{-1} h^{-1})	Ref.
BAIO/C_3N_4	300 W Xe lamp (λ > 420 nm)	535.9	This work
Reduced g-C_3N_4	300 W Xe lamp (λ > 420 nm)	460	[1]
$Bi_4O_5Br_2$/g-C_3N_4	300 W Xe lamp (λ > 420 nm)	124	[2]
$Cd_{0.6}Zn_{0.4}S$/g-C_3N_4	300 W Xe lamp (λ > 420 nm)	1098.5	[3]
C_3N_4/Mn/AB-CN	40 W LED lamp (λ = 427 nm)	410	[4]
NiS@g-C_3N_4	λ > 400 nm	400	[5]
B,Cs co-doped g-C_3N_4	λ > 420 nm	113	[6]
BP@CN	λ > 420 nm	540	[7]

C, O doped g-C_3N_4	$\lambda > 420$ nm	32.00	[8]

References

1. Z. D. Zhu, H. H. Pan, M. Murugananthan, J. Y. Gong and Y. R. Zhang, Visible light-driven photocatalytically active g-C_3N_4 material for enhanced generation of H_2O_2, *Appl. Catal. B Environ.*, 2018, **232**, 19-25.
2. X. S. Zhao, Y. Y. You, S. B. Huang, Y. X. Wu, Y. Y. Ma, G. Zhang and Z. H. Zhang, Z-scheme photocatalytic production of hydrogen peroxide over $Bi_4O_5Br_2$/g-C_3N_4 heterostructure under visible light, *Appl. Catal. B Environ*, 2020, **278**, 119251.
3. W. Y. Yu, Z. J. Zhu, C. H. Hu, S. Lin, Y. H. Wang, C. Y. Wang, N. Tian, Y. H. Zhang and H. W. Huang, Point-to-face Z-scheme junction $Cd_{0.6}Zn_{0.4}S$/g-C_3N_4 with a robust internal electric field for high-efficiency H_2O_2 production, *J. Mater. Chem. A*, 2023, **11**, 6384-6393.
4. P. Ren, T. Zhang, N. Jain, H. Y. V. Ching, A. Jaworski, G. Barcaro, S. Monti, J. Silvestre-Albero, V. Celorrio, L. Chouhan, A. Rokicińska, E. Debroye, P. Kuśtrowski, S. Van Doorslaer, S. Van Aert, S. Bals and S. Das, An atomically dispersed Mn-photocatalyst for generating hydrogen peroxide from seawater via the water oxidation reaction (WOR), *J. Am. Chem. Soc.*, 2023, **145**, 16584-16596.
5. X. Q. Yang, W. Wang, R. Ran, W. Zhou and Z. P. Shao, Recent advances in $Cs_2AgBiBr_6$-based halide double perovskites as lead-free and inorganic light absorbers for perovskite solar cells, *Energy & Fuels*, 2020, **34**, 10513-10528.
6. T. Mahvelati-Shamsabadi, H. Fattahimoghaddam, B.-K. Lee, H. Ryu and J. I. Jang, Caesium sites coordinated in boron-doped porous and wrinkled graphitic carbon nitride nanosheets for efficient charge carrier separation and transfer: Photocatalytic H_2 and H_2O_2 production, *Chem. Eng. J.*, 2021, **423**, 130067.
7. Y. Zheng, Z. H. Yu, H. H. Ou, A. M. Asiri, Y. L. Chen and X. C. Wang, Black phosphorus and polymeric carbon nitride heterostructure for photoinduced molecular oxygen activation, *Adv. Funct. Mater.*, 2018, **28**, 1705407.
8. S. Samanta, R. Yadav, A. Kumar, A. Kumar Sinha and R. Srivastava, Surface modified C, O co-doped polymeric g-C_3N_4 as an efficient photocatalyst for visible light assisted CO_2 reduction and H_2O_2 production, *Appl. Catal. B Environ.*, 2019, **259**, 118054.